*electronics*

MDPI

*Article*

# Research on Dynamic Response of Cold Rolling Mill with Dynamic Stiffness Compensation

**Xingdou Jia [1], Shen Wang [2], Xiaoqiang Yan [1,*], Lidong Wang [1] and Haipeng Wang [1]**

[1] School of Mechanical Engineering, University of Science and Technology Beijing, Beijing 100083, China
[2] Department of Mechanical Engineering and Mechanics, Lehigh University, Bethlehem, PA 18015, USA
* Correspondence: yanxq@ustb.edu.cn; Tel.: +86-186-0026-0898

**Abstract:** The vibration of the vertical system of a cold rolling mill is a major concern for factory production. In factory production, it is found that the thickness control system with dynamic stiffness compensation of the rolling mill has a significant impact on the rolling mill vibration. In this work, a mechanical hydraulic coupling vibration model of a cold rolling mill with a thickness control system with dynamic stiffness compensation was established. MATLAB/Simulink was used to simulate and analyze the vibration response characteristics of the mechanical structure of the rolling mill and mechanical hydraulic coupling system considering the dynamic stiffness compensation control mode and position control mode of the upper cylinder. We found that the control system changed the vibration response of the mechanical structure, and different control modes have different effects on the vibration response curve. When the rolling mill works in the vibration area, the thickness difference at the strip steel outlet would be larger. Considering the rolling mill vibration and strip surface quality, the excitation of the strip inlet thickness can be achieved by adjusting the dynamic stiffness compensation system and changing the rolling speed reasonably to achieve good vibration suppression and control effects.

**Keywords:** cold rolling mill; dynamic stiffness compensation; mechanical hydraulic coupling system; strip thickness excitation; dynamic response characteristics

check for updates

**Citation:** Jia, X.; Wang, S.; Yan, X.; Wang, L.; Wang, H. Research on Dynamic Response of Cold Rolling Mill with Dynamic Stiffness Compensation. *Electronics* **2023**, *12*, 599. https://doi.org/10.3390/electronics12030599

Academic Editor: Davide Astolfi

Received: 24 December 2022
Revised: 19 January 2023
Accepted: 20 January 2023
Published: 25 January 2023

**Copyright:** © 2023 by the authors. Licensee MDPI, Basel, Switzerland. This article is an open access article distributed under the terms and conditions of the Creative Commons Attribution (CC BY) license (https://creativecommons.org/licenses/by/4.0/).

## 1. Introduction

The vertical system vibration of a cold rolling mill is a common problem in factory production, and the vibration phenomena are also diverse, including forced vibration and self-excited vibration. Numerous studies have been focused on the vibration mechanism and the corresponding suppression methods.

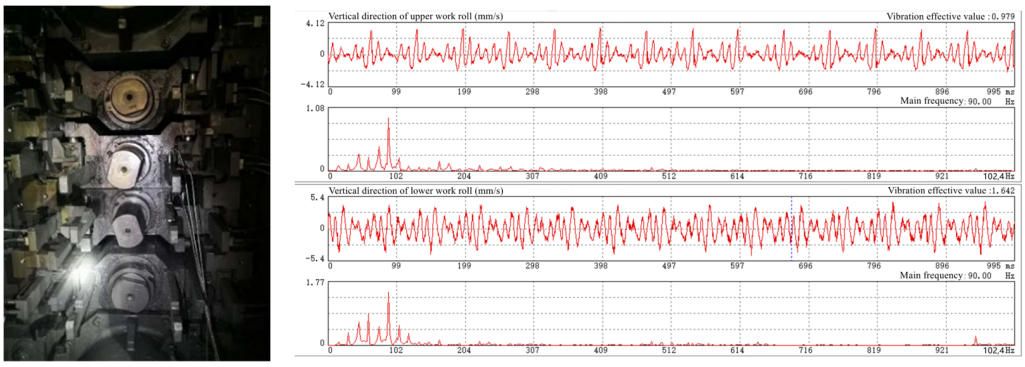
First of all, Li et al. [1] summarized and reviewed the research on cold rolling mill vibration. Yan et al. [2] found that the polygonal roll caused by the grinder would lead to the vibration of the cold rolling mill through vibration testing in the factory. Skripalenko et al. [3] analyzed the thickness fluctuation of strip steel and found that the rolling mill vibration was caused by the gear problem of the reduction box. The instability of rolling parameters is also an important reason for rolling mill vibration, besides external factors. Mehrabi et al. [4] established a linear spring mass model for the rolling mill by using the finite element method and analyzed the influence of the rolling parameters on vibration. Xu et al. [5] established a vertical nonlinear vibration model of the rolling mill based on the rolling force, and studied the nonlinear vibration characteristics of the rolling mill under multi-parameter excitation. Wang et al. [6] analyzed the influence of various process parameters on the vertical dynamic characteristics of the cold rolling mill.

PR Evans et al. [7] focused on the influence of the tension system on the first two inherent characteristics of the rolling mill. Qu et al. [8] analyzed the dynamic characteristics of the cold rolling mill frame with the finite element method, and they concluded that the rolling speed is a key factor for rolling mill vibration. Adam Bar et al. [9] established a

nonlinear vibration model of a continuous rolling mill based on strip steel coupling and studied the relationship between the strip steel speed and self-excited rolling vibration amplitude. Gao et al. [10–12] established a nonlinear dynamic model of rolling mill machinery and a rolling piece coupling system and calculated the conditions of rolling mill instability, so that they accurately predicted the limit rolling speed of rolling mill vibration. Yarita et al. [13] discussed the influence of lubrication on roll stability in detail and analyzed the vibration mechanism of a cold rolling mill. Noriki et al. [14] proposed a mixed lubrication control method, which can make rolling more stable and improve the rolling speed through simulation analysis. Yang et al. [15] established a rolling vibration coupling model based on the lubrication principle and discussed the relationship between the process parameters and rolling stability.

Wei et al. [16] found that a change in the roll gap oil film caused rolling mill vibration. They were able to optimize the lubrication process to suppress the vibration and improve the rolling speed. The dynamic characteristics of the rolling mill itself are another important aspect to study regarding the rolling mill vibration. Liu et al. [17] coupled the dynamic rolling process and rolling mill structure vibration model to the continuous rolling mill regenerative flutter model, and analyzed the stability of the model in detail. Liu et al. [18] established a nonlinear model based on the dynamic rolling force, and studied the amplitude frequency characteristics and bifurcation behavior of rolling mill vibration. The coupling dynamic characteristics of the rolling mill have attracted more and more attention. Cai et al. [19] established a hydraulic system model of the cold rolling mill, and obtained the dynamic characteristics of the actual rolling mill system by analyzing the time domain and frequency domain. Pen et al. [20] established a multi-directional coupled vibration model of the rolling mill, and studied the relationship between roll vibration and strip steel characteristics from the perspective of thickness control. Xu et al. [21] established a mechanical hydraulic coupling vibration model, and found that a robust controller has a better vibration suppression effect than a PID controller. Hou et al. [22] proposed a method to suppress the mill hydraulic coupling vibration by adjusting the response time of the servo valve. Zhu et al. [23] studied the excitation mechanism of strip thickness fluctuation and hardness fluctuation on rolling mill vibration, but they did not provide targeted vibration suppression measures. Therefore, the research on rolling mill vibration is not perfect, and there are many aspects to be further studied.

However, the impact of dynamic stiffness compensation on the vibration of the cold rolling mill has not been studied in relevant articles so far. During the vibration test in the factory, as shown in Figure 1, we found that after stopping the dynamic stiffness compensation of the rolling mechanism, the effective value of the upper work roll's vibration did not change notably, while the effective value of the lower work roll's vibration doubled. This phenomenon of vibration change has led to new ideas for restraining rolling mill vibration.




(**a**) (**b**)

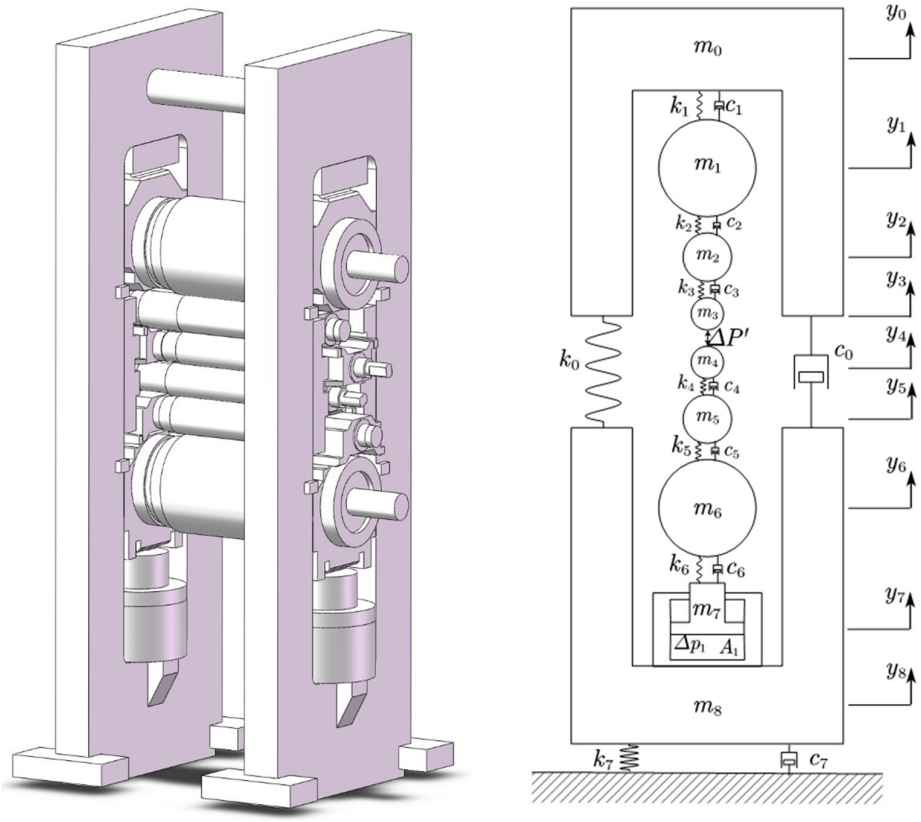
**Figure 1.** On−site vibration test diagram of upper and lower work rolls of cold rolling mill: (**a**) testing diagram in the factory; (**b**) spectrum diagram of upper and lower work roll test.

In order to verify whether the vibration of a rolling mill can be suppressed by adjusting the dynamic stiffness compensation, it is necessary to explore the influence of dynamic stiffness compensation on rolling mill vibration and strip surface quality. According to the research results and the actual situation in production, adjusting the dynamic stiffness compensation of the rolling mill may also become one of the most feasible methods for the company to suppress vibration.

## 2. Modeling of Vertical Vibration System of Rolling Mill

### *2.1. Establishment of Vibration Model*

The cold rolling mill of a steel plant is a six-high-mill, and the mechanical structure of the mill is shown in Figure 2a. According to the mass and stiffness characteristics of all parts of the rolling mill, the vertical system of the rolling mill is simplified as a vertical vibration model with 9 degrees of freedom, as shown in Figure 2b.




(**a**) (**b**)

**Figure 2.** Mechanical structure diagram and vibration model diagram of vertical system of rolling mill: (**a**) three-dimensional model diagram of mechanical structure of cold rolling mill; (**b**) equivalent vertical vibration model diagram of cold rolling mill.

The vibration differential Equations (1)–(9) established according to the spring mass vibration model in Figure 2 are as follows.

$$m_0\ddot{y}_0 + c_0(\dot{y}_0 - \dot{y}_8) + c_1(\dot{y}_0 - \dot{y}_1) + k_0(y_0 - y_8) + k_1(y_0 - y_1) = 0 \quad (1)$$

$$m_1\ddot{y}_1 - c_1(\dot{y}_0 - \dot{y}_1) + c_2(\dot{y}_1 - \dot{y}_2)_1 - k_1(y_0 - y_1) + k_2(y_1 - y_2) = 0 \quad (2)$$

$$m_2\ddot{y}_2 - c_2(\dot{y}_1 - \dot{y}_2) + c_3(\dot{y}_2 - \dot{y}_3) - k_2(y_1 - y_2) + k_3(y_2 - y_3) = 0 \quad (3)$$

$$m_3\ddot{y}_3 - c_3(\dot{y}_2 - \dot{y}_3) - k_3(y_2 - y_3) = \Delta P \quad (4)$$

$$m_4\ddot{y}_4 + c_4(\dot{y}_4 - \dot{y}_5) + k_4(y_4 - y_5) = -\Delta P \quad (5)$$

$$m_5\ddot{y}_5 - c_4(\dot{y}_4 - \dot{y}_5) + c_5(\dot{y}_5 - \dot{y}_6) - k_4(y_4 - y_5) + k_5(y_5 - y_6) = 0 \quad (6)$$

$$m_6\ddot{y}_6 - c_5(\dot{y}_5 - \dot{y}_6) + c_6(\dot{y}_6 - \dot{y}_7) - k_5(y_5 - y_6) + k_6(y_6 - y_7) = 0 \quad (7)$$

$$m_7\ddot{y}_7 - c_6(\dot{y}_6 - \dot{y}_7) - k_6(y_6 - y_7) = \Delta p_1 A_1 \quad (8)$$

$$m_8\ddot{y}_8 - c_0(\dot{y}_0 - \dot{y}_8) + c_7\dot{y}_8 - k_0(y_0 - y_8) + k_7 y_8 = -\Delta p_1 A_1 \quad (9)$$

where $m_0$ is the total mass of the upper part of the arch, the support roll bearing seat and the adjusting step pad; $m_1$ is the mass of the upper support roll; $m_2$ is the mass of the upper intermediate roll and its bearing seat; $m_3$ is the mass of the upper working roll and its bearing seat; $m_4$ is the mass of the lower work roll and its bearing seat; $m_5$ is the mass of the lower intermediate roll and its bearing seat; $m_6$ is the mass of the lower support roll; $m_7$ is the total mass of the lower support roll bearing seat and the hydraulic cylinder piston; $m_8$ is the total mass of the lower part of the arch and the rigid body of the hydraulic cylinder. $k_0$ and $c_0$ are the equivalent stiffness and damping of the arch column, respectively; $k_1$ and $c_1$ are the equivalent stiffness and damping of the upper support roll bearing pedestal, respectively; $k_2$ and $c_2$ are the equivalent stiffness and damping between the upper backup roll and the upper intermediate roll, respectively; $k_3$ and $c_3$ are the equivalent stiffness and damping between the upper intermediate roll and the upper work roll, respectively; $k_4$ and $c_4$ are the equivalent stiffness and damping between the lower intermediate roll and the lower work roll, respectively; $k_5$ and $c_5$ are the equivalent stiffness and damping between the lower backup roll and the lower intermediate roll, respectively; $k_6$ and $c_6$ are the equivalent stiffness and damping of the lower support roll bearing pedestal, respectively; $k_7$ and $c_7$ are the equivalent stiffness and damping of the arch anchor bolt, respectively; $\Delta P'$ is the dynamic rolling force between roll gaps considering roll flattening; $\Delta p_1$ is the dynamic pressure of the rodless cavity of the hydraulic upper cylinder; $A_1$ is the rodless cavity area of the hydraulic press cylinder.

### *2.2. Vibration System Parameters*

According to the factory equipment drawings, the mass parameters in the vibration system can be obtained after three-dimensional modeling, and the stiffness parameters can be calculated according to the equipment parameters. The mass parameters of the vibration system are shown in Table 1, the equipment and process parameters are shown in Table 2, and the damping ratio is set to 0.01. Part of the stiffness in the vibration system is calculated by the following Formula (10) [13].

$$k = \frac{\pi LE}{2(1-\mu^2)\{0.1182 + \ln EL(D_1 + D_2) - \ln 2P(1-\mu^2)\}} \quad (10)$$

Here, $L$ is the contact length between rolls; $E$ is the elastic modulus of the roll; $\mu$ is Poisson's ratio; $D_1$ and $D_2$, respectively, represent the diameters of the two rolls in contact; $P$ is the rolling pressure between rolls.

**Table 1.** Parameters of equivalent mass of rolling mill (T).

| $m_0$ | $m_1$ | $m_2$ | $m_3$ | $m_4$ | $m_5$ | $m_6$ | $m_7$ | $m_8$ |
|---|---|---|---|---|---|---|---|---|
| 88.686 | 21.641 | 5.853 | 4.461 | 4.455 | 5.829 | 21.641 | 19.514 | 91.074 |

From Formula (10), we can obtain $k_2 = k_5 = 4535$ T/mm and $k_3 = k_4 = 4810$ T/mm.

The contact stiffness between the upper and lower work rolls is $k_P = 4842$ T/mm. According to the test in the factory, the total nominal stiffness of the rolling mill is $K = 400$ T/mm.

The relationships among the calibration stiffness of the rolling mill and stiffness in the vibration system are as shown in Equation (11).

$$\frac{1}{K} = \frac{1}{k_0} + \frac{1}{k_1} + \frac{1}{k_2} + \frac{1}{k_3} + \frac{1}{k_4} + \frac{1}{k_5} + \frac{1}{k_6} + \frac{1}{k_P} + \frac{V_1}{2\beta_e A_1^2} \quad (11)$$

Here, $V_1$ is the volume of the hydraulic cylinder; $\beta_e$ is the effective bulk elastic modulus of the hydraulic oil.

**Table 2.** Factory equipment and process parameters.

| Name | Value | Unit | Name | Value | Unit |
|---|---|---|---|---|---|
| $L$ | 1450 | mm | $h_0$ | 0.55 | mm |
| $E$ | 210 | Gpa | $h_1$ | 0.5 | mm |
| $\mu$ | 0.3 | | $\sigma$ | 900 | Mpa |
| $B$ | 1000 | mm | $\tau_b$ | 173.6 | Mpa |
| $R$ | 200 | mm | $\tau_f$ | 50 | Mpa |
| $\eta$ | 0.05 | | $A_1$ | 0.623 | $m^2$ |
| $V_1$ | 0.06853 | $m^3$ | $\beta_e$ | 1280 | Mpa |

Because $k_0 = 5348$ T/mm, we can obtain $k_1 = k_6 = 3571$T/mm. In addition, $k_7 = 23,797.5$ T/mm.

The cold rolling force formula is as shown in (12)–(17) [24].

$$P = Bl_c{}'p_m = Bl_c{}'Q_pK_TK_B/1000 \tag{12}$$

$$l'_c = \sqrt{R' \triangle h} \tag{13}$$

$$R' = R(1 + 2.2 \times 10^{-5}\frac{P}{B \triangle h}) \tag{14}$$

$$Q_p = 1.08 + 1.79\eta\varepsilon\sqrt{1-\varepsilon}\sqrt{\frac{R'}{h_1}} - 1.02\varepsilon \tag{15}$$

$$\varepsilon = \frac{\Delta h}{h_0} = \frac{h_0 - h_1}{h_0} \tag{16}$$

$$K_T = 1 - \frac{0.7\tau_b + 0.3\tau_f}{K_B} \tag{17}$$

Here, $B$ represents the width of the rolled piece; $l_c{}'$ represents the contact arc length of the roll after elastic flattening; $R$ is the roll radius; $R'$ is the radius of the roll after elastic flattening; $Q_p$ is the friction stress state coefficient of the strip steel and roll after elastic flattening; $\eta$ is the friction coefficient; $h_0$ is the inlet thickness; $h_1$ is the outlet thickness; $K_T$ is the tension influence coefficient; $K_B$ is the deformation resistance after considering the width influence coefficient, $K_B = 1.15\sigma$; $\sigma$ is the material deformation resistance considering work hardening; $\varepsilon$ is the reduction rate; $\tau_b$ represents the post-tension of the strip steel; $\tau_f$ represents the tension before the strip steel.

The rolling force fluctuation is determined by the inlet thickness and the outlet thickness, without considering the hardness of the strip steel and the tension fluctuation before and after. Then, the dynamic rolling force is as shown in (18)–(19).

$$\Delta P = \frac{\partial P}{\partial h_0}\Delta h_0 - \frac{\partial P}{\partial h_1}\Delta h_1 = \frac{\partial P}{\partial h_0}\Delta h_0 - Q\Delta h_1 \tag{18}$$

$$\Delta P' = \frac{\partial P}{\partial h_0}\Delta h_0 - \frac{Qk_P}{Q + k_P}\Delta h_1 \tag{19}$$

Bringing the equipment and process parameters into Equations (12)–(18), we can obtain $\frac{\partial P}{\partial h_0} = 2570$ T/mm, $\frac{\partial P}{\partial h_1} = 2560$ T/mm.

The outlet thickness fluctuation of the strip steel is as shown in Equation (20).

$$\Delta h_1 = \frac{k_p}{\partial P/\partial h_1 + k_p}(y_3 - y_4) \tag{20}$$

## 3. Modeling of Thickness Control System

### *3.1. Model of Thickness Control System with Variable Stiffness Compensation for Rolling Mill*

According to the rolling principle of the rolling mill, the ideal rolling thickness of strip steel is as shown in Formula (21).

$$h_1 = S_0 + \frac{P_0}{K} \tag{21}$$

where $S_0$ is the preset roll gap value; $P_0$ is the set rolling force.

The core algorithm of the variable stiffness thickness control system is as shown in Formula (22) [25].

$$h = S + C\frac{P}{K} \tag{22}$$

Here, $C$ is the variable stiffness coefficient. The variable stiffness control system introduces variable stiffness coefficient $C$ based on the original system.

When the thickness of the inlet strip steel changes, the corresponding rolling force variation is $\Delta P$. The theoretical thickness change is as shown in Formula (23), and the actual thickness change is the value when $C = 1$.

$$\Delta h = C\frac{\Delta P}{K} \tag{23}$$

In order to eliminate this thickness deviation, according to the P-H diagram analysis, the thickness difference of the strip steel can be eliminated by adjusting the hydraulic cylinder position value to change the roll gap. The relationship between hydraulic cylinder adjustment amount $\Delta S^*$ and roll gap change amount $\Delta h$ is as shown in Formula (24).

$$\Delta S^* = \frac{K + M}{K}\Delta h \tag{24}$$

$$M = \frac{\partial P}{\partial h_1} \tag{25}$$

We add $\Delta S^*$ and the original magnetic ruler position as the given value of the magnetic ruler position for closed-loop control. After adjustment, the thickness deviation of the strip steel can be expressed as in Formula (26).

$$\Delta h' = \Delta h|_{C=1} - \Delta S^*\frac{K}{K+M} = \frac{\Delta P}{K} - C\frac{\Delta P}{K} = \frac{\Delta P}{\frac{K}{1-C}} = \frac{\Delta P}{K_e} \tag{26}$$

where $K_e$ is the equivalent stiffness of the rolling mill.

Equation (26) is the basic equation of rolling mill dynamic stiffness control, i.e., the equivalent rolling mill stiffness $K_e$ is changed by adjusting the compensation coefficient $C$.

When $C = 1$, $K_e = \infty$, $\Delta h' = 0$, and this means that the rolling mill has super-hard stiffness, and, theoretically, there is no thickness difference for the strip steel.

When $C = 0$, $K_e = K$, $\Delta h' = \frac{\Delta P}{K}$, it means that the rolling mill has natural stiffness, and the thickness difference of the strip steel is caused by the quality of the inlet strip steel.

### *3.2. Modeling of Hydraulic Control System*

The hydraulic screw-up system of the cold rolling mill uses the structure of the hydraulic cylinder driven by a force motor valve. First, the power amplifier outputs a current to drive the solenoid coil of the force motor, so that the solenoid coil generates electromagnetic force to drive the valve core to move, thus controlling the oil inlet and outlet of the rodless cavity of the hydraulic cylinder. At the same time, the rod cavity maintains a constant back pressure.

The relationship between the electromagnetic coil current and electromagnetic force equation is shown in Formula (27) below.

$$F = B\pi dNi \tag{27}$$

where $F$ is the electromagnetic force generated by the electromagnetic coil; $B$ is the magnetic induction intensity around the coil of the permanent magnet; $d$ is the diameter of the electromagnetic coil; $N$ is the number of turns of the electromagnetic coil.

The force balance differential equation of the counter-force motor valve core is as shown in Formula (28).

$$F = m\frac{d^2x_v}{dt^2} + (B_n + B_s)\frac{dx_v}{dt} + (k_v + k_f)x_v \tag{28}$$

Here, $m$ is the mass of the valve element and solenoid coil; $x_v$ is the spool displacement; $B_n$ and $B_s$ are the viscous damping coefficient of the system and the damping coefficient generated by the transient hydrodynamic force, respectively. The damping coefficient of the valve element is generally small and can be ignored; here, the total damping coefficient is taken as 0.001; $k_v$ is the stiffness of the valve core centering spring; $k_f$ is the steady hydraulic stiffness of the valve element, which is equivalent to the spring stiffness.

Formulas (27) and (28) are transformed by the Laplace transform, and the transfer function of the spool displacement and driving current is obtained after calculation, as shown in Formula (29).

$$G_1(s) = \frac{x_v(s)}{i(s)} = \frac{B\pi dN}{ms^2 + (B_n + B_s)s + (k_v + k_f)} \tag{29}$$

The flow pressure equation of the FMV valve is shown in Formula (30) [26].

$$q_1 = \begin{cases} C_d W x_v \sqrt{\frac{2}{\rho}(p_s - p_1 - \Delta p_1)} & x_v \geq 0 \\ C_d W x_v \sqrt{\frac{2}{\rho}(p_1 + \Delta p_1)} & x_v < 0 \end{cases} \tag{30}$$

where $C_d$ is the flow coefficient; $W$ is the gradient of the valve port area; $p_s$ is the oil source pressure; $\rho$ is the oil density; $p_1$ is the steady pressure of the rodless cavity of the hydraulic cylinder.

We linearize the flow pressure equation of the FMV valve at the zero position to obtain Formula (31).

$$\Delta q_1 = K_q \Delta x_v - K_c \Delta p_1 \tag{31}$$

Here, $K_q$ is the servo valve flow gain; $K_c$ is the flow pressure coefficient of the servo valve.

The flow continuity equation of the rodless cavity of the hydraulic pressure cylinder is shown in Formula (32).

$$q_1 = A_1\frac{dX_V}{dt} + C_{ip}(p_1 - p_2) + C_{ep}p_1 + \frac{V_1}{\beta_e}\frac{dp_1}{dt} \tag{32}$$

$$X_V = y_7 - y_8 \tag{33}$$

Here, $X_V$ is the displacement of the hydraulic cylinder; $q_1$ is the flow into or out of the hydraulic upper cylinder; $C_{ip}$ is the internal leakage coefficient of the upper cylinder; $C_{ep}$ is the external leakage coefficient of the upper cylinder; $\beta_e$ is the effective bulk modulus of elasticity, which is related to the oil pressure; $V_1$ is the volume of the rodless cavity of the hydraulic pressure cylinder.

Since $C_{ip} \approx 0$, $C_{ep} \approx 0$, simplified as Formula (32), is simplified as Formula (34):

$$q_1 = A_1\frac{dX_V}{dt} + \frac{V_1}{\beta_e}\frac{dp_1}{dt} \tag{34}$$

The hydraulic system parameters are shown in Table 3.

**Table 3.** Hydraulic system parameters.

| Name | Value | Unit | Name | Value | Unit |
|---|---|---|---|---|---|
| $m$ | 0.148 | Kg | $p_s$ | 20.6 | Mpa |
| $k_v + k_f$ | 59,090 | N/m | $p_1$ | 7.9 | Mpa |
| $i_{\max}$ | 10 | A | $\rho$ | 870 | Kg/m$^3$ |
| $x_{v\max}$ | 3 | mm | $K_c$ | 0.1367 | L/min·Mpa |
| $C_d$ | 0.61 | | $K_q$ | 50 | L/min·mm |
| $W$ | 47.124 | mm | $B\pi dN$ | 17.727 | N/A |

Combining the vertical vibration system model of the rolling mill and the thickness control system with the dynamic stiffness compensation model, a rolling mill mechanical hydraulic coupling vibration model is jointly established, as shown in Figure 3 below.

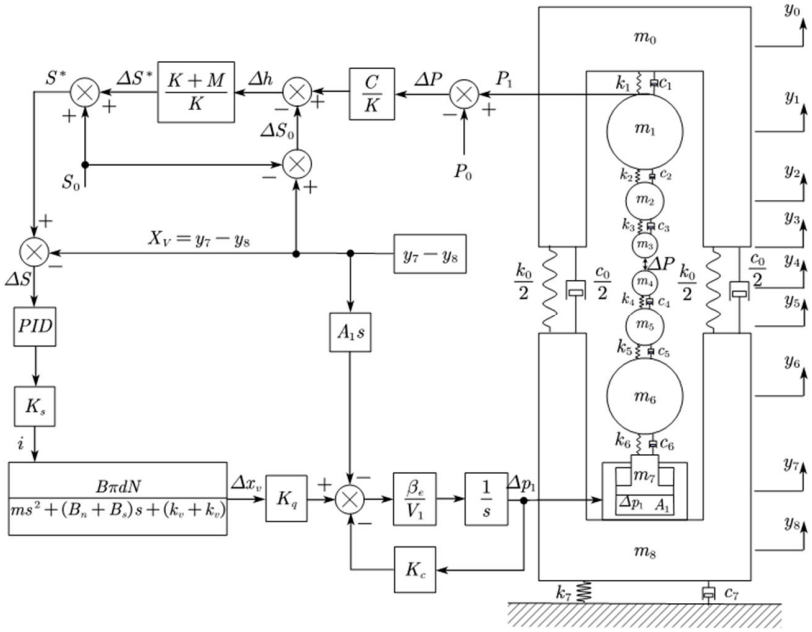



**Figure 3.** Mechanical hydraulic coupling vibration model of vertical system of rolling mill.

It can be seen from Figure 3 that the thickness control system of the rolling mill adopts a double closed-loop control mode. The outer is a thickness loop; it calculates the change in roll gap according to the rolling force, and the adjustment of the hydraulic cylinder is calculated in real time from the change in roll gap. Then, the roll gap is kept unchanged by adjusting the hydraulic cylinder. The inner is a position loop; the adjustment amount of the hydraulic cylinder calculated by the thickness loop is used as the given signal of the hydraulic cylinder position. After comparing this with the feedback signal of the hydraulic cylinder position sensor, the PID controller controls the servo valve to realize the position control of the hydraulic cylinder.

In order to minimize the fluctuation of the strip outlet thickness during rolling mill operation, generally, $C = 1$. Under some working conditions, the thickness loop will also be closed, i.e., $C = 0$, so that the mill can work in the position ring control mode.

Without considering the influence of the control system on the mechanical structure, the oil in the hydraulic cylinder would be neither flowing in nor flowing out by closing the servo valve. The hydraulic oil can be regarded as a hydraulic spring. The spring stiffness Formula (35) is as shown below:

$$K_h = \frac{2\beta_e A_1^2}{V_1} \tag{35}$$

At this time, the vibration Equations (8) and (9) become (36) and (37):

$$m_7\ddot{y}_7 - c_6(\dot{y}_6 - \dot{y}_7) - k_6(y_6 - y_7) + K_h(y_7 - y_8) = 0 \tag{36}$$

$$m_8\ddot{y}_8 - c_0(\dot{y}_0 - \dot{y}_8) + c_7\dot{y}_8 - k_0(y_0 - y_8) + k_7y_8 - K_h(y_7 - y_8) = 0 \tag{37}$$

### *3.3. MATLAB/Simulink Simulation Model of Vertical System of Rolling Mill*

Regardless of the thickness control system of the rolling mill, the MATLAB/Simulink vibration model of the rolling mill mechanical system is as shown in Figure 4.

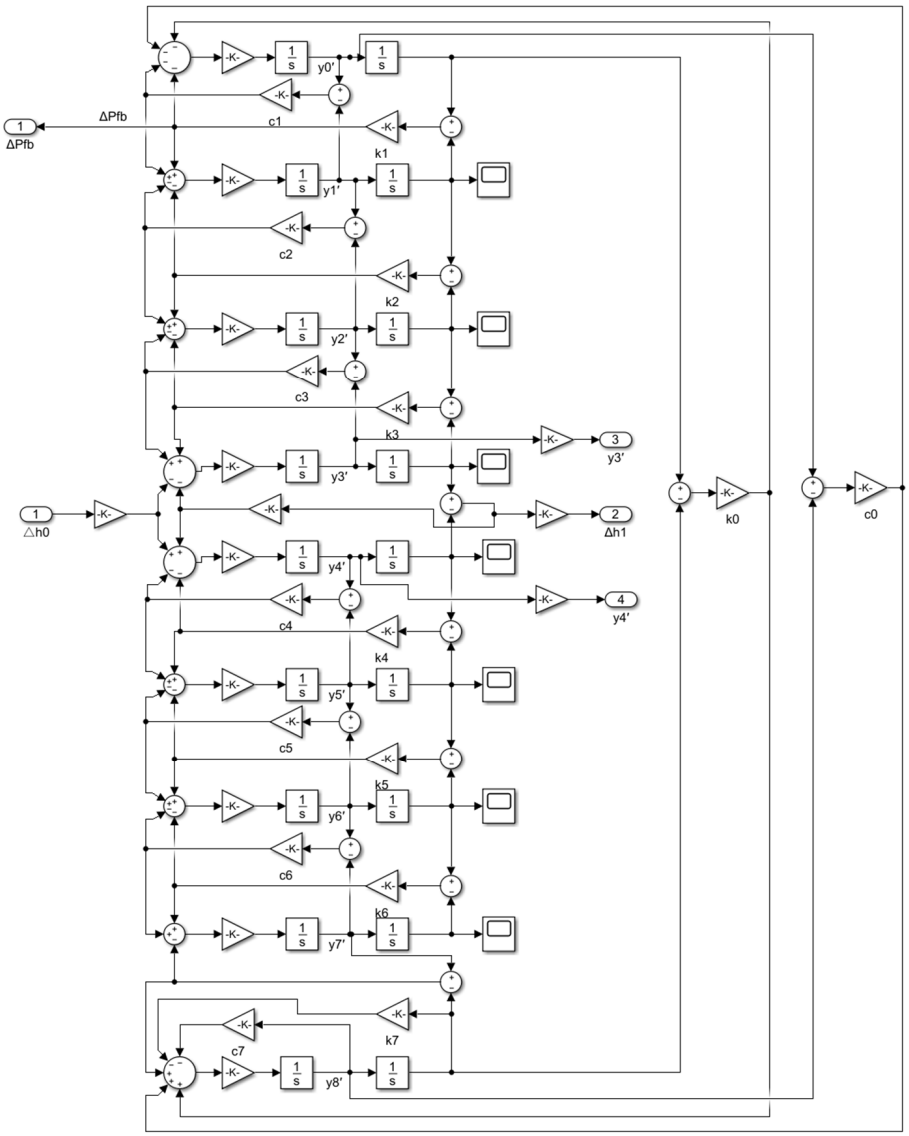



**Figure 4.** MATLAB/Simulink simulation diagram of mechanical vibration system of rolling mill.

According to Figure 2, we remove the steady-state components of the rolling mill system, and make $P_0$ and $S_0$ zero. The established MATLAB/Simulink simulation model of rolling mill hydraulic coupling vibration is shown in Figure 5.

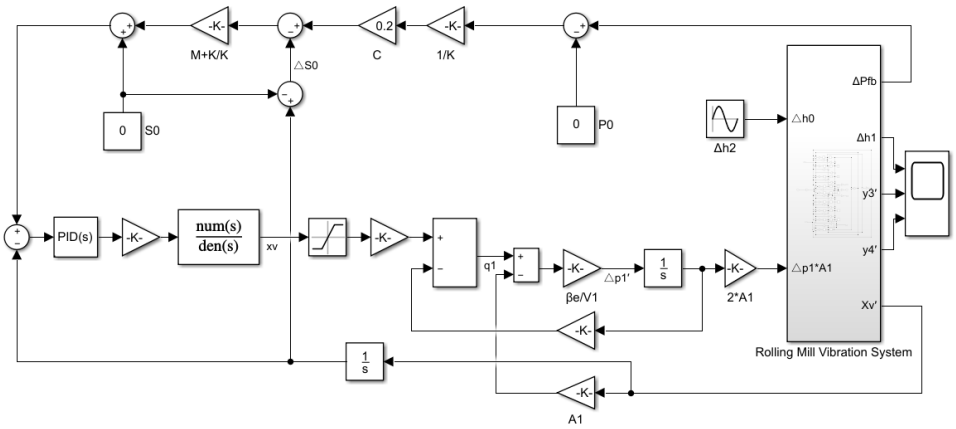



**Figure 5.** MATLAB/Simulink simulation diagram of mill hydraulic coupling vibration.

In order to verify the accuracy of the simulation parameters, we compared the step responses of the hydraulic cylinder position between the simulation model and factory test. In the factory test, the roll seam strip was removed, and 200 T pressure was applied through the hydraulic pressing system. Then, the position step signals of 20 μm were respectively given to the hydraulic cylinders on both sides at the same time. The given signals and response signals are shown in Figure 6.

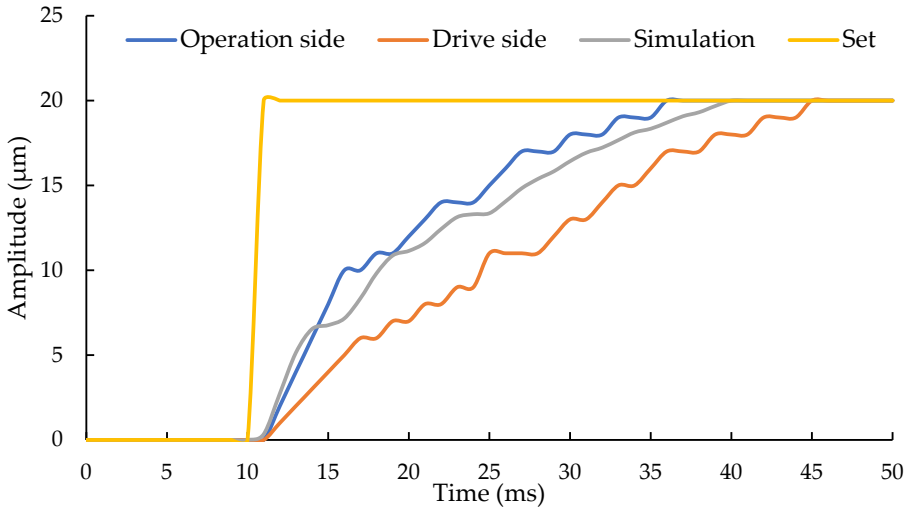



**Figure 6.** Step response curve of simulation model and factory test.

It can be seen from Figure 5 that the response speed of the hydraulic screw-up systems on both sides of the rolling mill is different, and the response speed of the operation side is obviously faster than that of the drive side. The response speed of the simulation system is between the operation side and the drive side, which is basically equal to the average speed of both sides. This shows that the parameters of the simulation system are consistent with the actual equipment. Therefore, we can conclude that the simulation results are accurate.

## 4. Simulation Analysis of Coupling Model

### *4.1. Vibration Response Analysis of Rolling Mill*

Suppose that there is a periodic thickness fluctuation at the entrance of the rolling mill, the amplitude of which is $A$, and the wavelength is $\lambda$. The thickness excitation at different rolling speeds shows different frequencies. The relationship between the excitation frequency and the wavelength is shown in Formula (38).

$$f = \frac{v}{\lambda} \tag{38}$$

where $v$ is the rolling speed.

Set $A$ = 3 μm and $f$ = 1–200 Hz in the simulation system. When $C$ = 1 and the excitation frequency is equal to 50 Hz and 150 Hz, respectively, the vibration time–frequency diagram of the upper and lower work rolls is as shown in Figures 7 and 8.

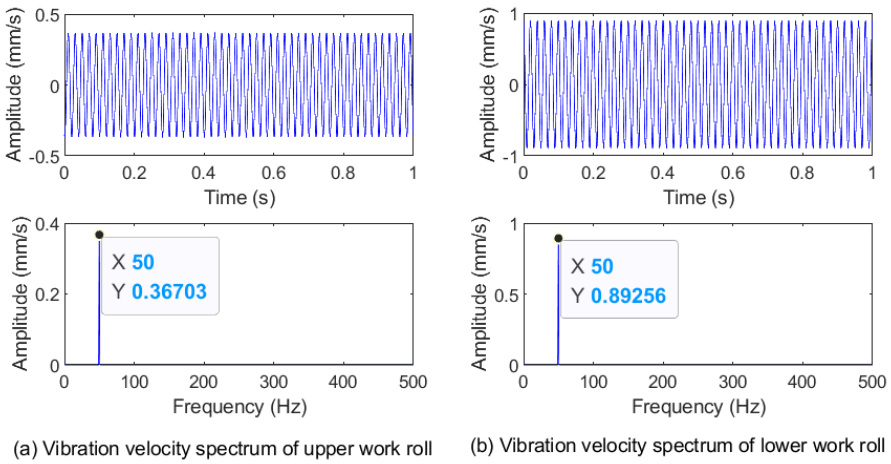



**Figure 7.** Rolling mill vibration spectrum at $C$ = 1, $f$ = 50 Hz.

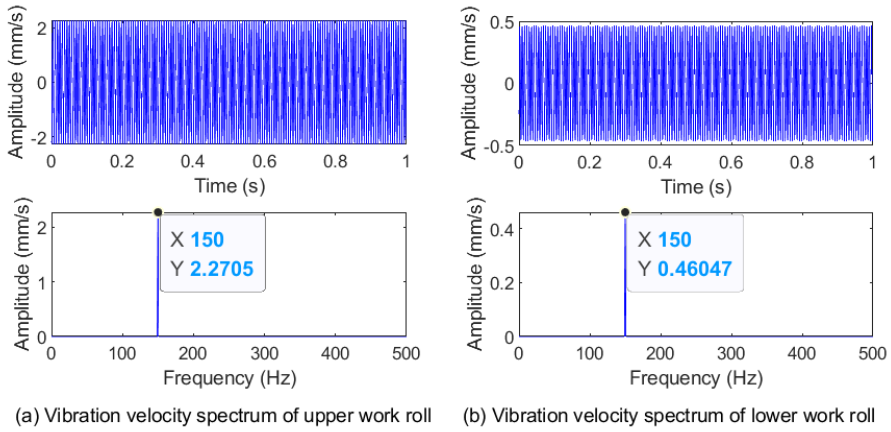



**Figure 8.** Rolling mill vibration spectrum at $C$ = 1, $f$ = 150 Hz.

The vibration frequency of the upper and lower work rolls is consistent with the excitation frequency of the strip steel, but the vibration amplitude is different. When the excitation frequency is 50 Hz, the vibration amplitude of the lower work roll is larger than that of the upper work roll. At 150 Hz, the vibration situation is completely reversed.

The vibration velocity responses of the upper and lower work roll in the vertical system of the rolling mill under the condition of $C$ = 1, $C$ = 0 and with the servo valve closed were recorded, respectively, as shown in Figures 9 and 10.

It can be seen from Figures 9 and 10 that the upper work roll and lower work roll continue to vibrate in the full frequency band as a result of the excitation of the strip steel inlet thickness, but the vibration response curves are not exactly the same. When the servo valve is closed, the upper work roll has two resonant frequencies of 82 Hz and 138 Hz, while the lower work roll has two resonant frequencies of 89 Hz and 133 Hz. After the introduction of the hydraulic pressure control system, the mechanical natural frequency of the vertical system of the rolling mill will change. At this time, the resonance frequency of the upper work roll and lower work roll will change to 80 Hz and 118 Hz, reducing the original resonance frequency of the mechanical system. When $C$ = 1, the resonance frequency of the upper work roll and lower work roll becomes 85 Hz and 119 Hz. When $C$ = 1, the resonance frequency of the upper and lower work rolls becomes 85 Hz and 119 Hz, which

is close to the natural frequency of the former case, but the vibration amplitude in some frequency bands is significantly different. The vibration amplitudes of the upper and lower work roll in the three states are different in different frequency bands. In the range below 100 Hz, the vibration of the lower work roll is relatively strong. In the range of 100–200 Hz, the vibration of the upper work roll is more severe.

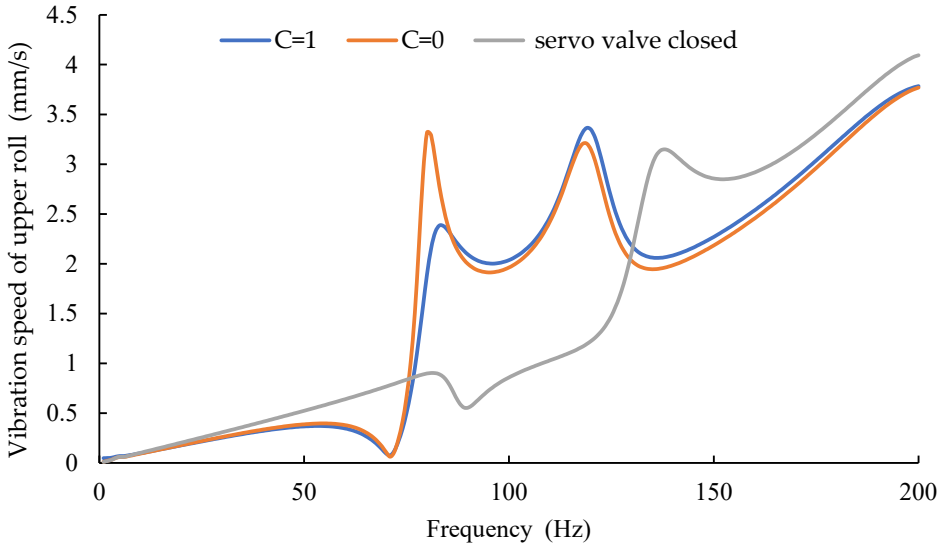



**Figure 9.** Amplitude frequency diagram of vibration speed of upper work roll.

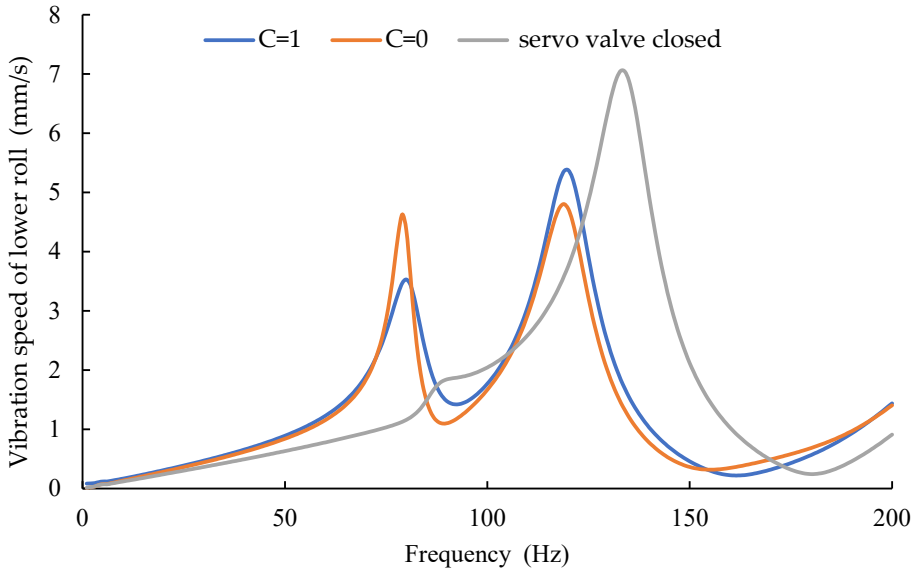



**Figure 10.** Amplitude frequency diagram of lower work roll vibration speed.

### *4.2. Strip Surface Quality Analysis*

The rolling mill will not only have different vibration responses in different working modes, but will also have different control effects on the thickness difference of the rolled steel. The thickness fluctuation curves of the outlet strip steel are shown in Figure 11 below.

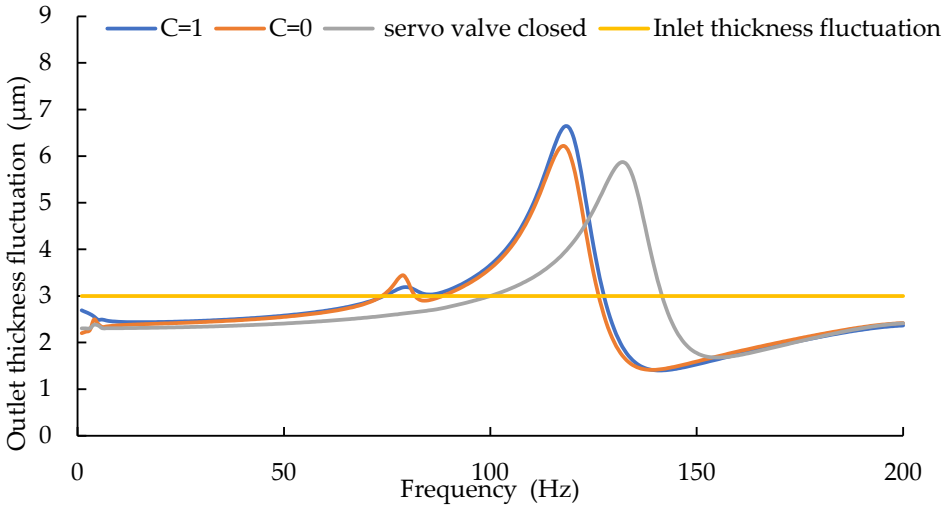



**Figure 11.** Thickness fluctuation diagram of strip steel at the inlet and outlet of rolling mill.

It can be seen from Figure 9 that the thickness control effect of the rolling mill on the strip steel is different in different working conditions. The outlet thickness fluctuation of the strip steel is also different under the excitation of the inlet thickness at different frequencies. In most frequency bands, the outlet thickness fluctuation is less than the inlet thickness fluctuation, which can lead to the ideal control effect. However, when the excitation frequency of the strip steel meets the natural frequency of the mill, the rolling mill will have strong vibration, which will cause the outlet thickness fluctuation to be greater than the inlet thickness fluctuation, and worsen the quality of the strip steel.

When the excitation frequency of the strip steel to the rolling mill is lower than 120 Hz, the rolling mill should close the servo valve for rolling to obtain the best surface quality of the strip steel. However, when the excitation frequency is greater than 120 Hz, the rolling mill should be placed into the hydraulic control system.

Above all, the vibration of the rolling mill is closely related to the control ability of the thickness difference of the strip steel. When the vibration of the rolling mill is in the relatively stable frequency band, the thickness control system can cause the thickness difference of the strip steel at the exit to be less than that at the entrance. However, when the rolling mill vibration is in the intense frequency band, the surface quality of the strip steel will become worse. Since the vibration frequency of the rolling mill is related to the rolling speed, the quality of the strip steel can also be improved by reasonably changing the rolling speed to avoid the resonance of the rolling mill.

## 5. Conclusions

(1) When the thickness fluctuation of the strip steel excites the rolling mill, the rolling mill will produce the same frequency vibration. At the same vibration frequency, the vibration amplitude of different parts of the rolling mill is different; moreover, with the change in vibration frequency, the vibration amplitude will also change.

(2) The resonance frequency of the rolling mill hydraulic coupling system considering the hydraulic screw-up control system is different from that of the rolling mill's mechanical structure itself, and the influence of different control modes on the resonance frequency of the rolling mill vertical system is also different.

(3) The rolling mill dynamic stiffness compensation thickness control system can more effectively control the outlet thickness fluctuation of strip steel in some frequency bands, but it cannot completely eliminate the outlet thickness fluctuation of the strip steel. When the excitation of strip steel renders the mill resonant, the outlet thickness fluctuation will be greater.

(4) When the excitation frequency of the strip steel to the rolling mill is in a different vibration range, the rolling mill can switch between different control modes to allow the

excitation frequency to avoid the natural frequency of the rolling mill. This can reduce the vibration amplitude of the rolling mill and obtain better strip surface quality simultaneously.

(5) For the rolling mill vibration caused by the excitation of the strip steel, the excitation frequency of the rolling mill can be changed by changing the rolling speed, so as to avoid the rolling resonance zone and improve the surface quality of the strip steel.

**Author Contributions:** Conceptualization, X.J.; methodology, X.J. and X.Y.; software, X.J.; validation, X.J., S.W., L.W. and H.W.; formal analysis, S.W.; investigation, L.W.; data curation, H.W.; writing—original draft preparation, X.J.; writing—review and editing, X.Y., L.W. and H.W.; visualization, X.J.; supervision, X.Y.; project administration, S.W. and X.Y.; funding acquisition, X.Y. All authors have read and agreed to the published version of the manuscript.

**Funding:** This work is supported by the National Natural Science Foundation of China (Grant No. 51775038).

**Data Availability Statement:** The data used to support the findings of this study are available from the corresponding author upon request.

**Conflicts of Interest:** The authors declare no conflict of interest.

## References

1. Li, X.; Chao, L.; Chen, F.; Zhang, D. Review and prospect of theoretical studies on vertical vibration in tandem cold rolling mill. *Steel Roll.* **2022**, *39*, 1–12. [CrossRef]
2. Yan, X.Q.; Zhang, Y. Research on vibration reason of reversing cold mill. *J. Vib. Shock.* **2010**, *29*, 231–234. (In Chinese)
3. Skripalenko, M.N.; Ashikhmin, D.A.; Sidorov, A.A.; Yang, X. Wavelet analysis of fluctuations in the thickness of cold-rolled strip. *Metallurgist* **2013**, *57*, 606–611.
4. Mehrabi, R.; Salimi, M.; Ziaei-Rad, S. Finite element analysis on chattering in cold rolling and comparison with experimental results. *J. Manuf. Sci. Eng.* **2015**, *137*, 061013. [CrossRef]
5. Xu, T.; Hou, D.-X.; Sun, Z.-N.; Guo, D.-W. Vibration characteristics of multi-parametric excitations and multi-frequency external excitations of rolling mill under entry thickness fluctuation of strip. *J. Iron Steel Res. Int.* **2020**, *27*, 517–527. [CrossRef]
6. Wang, Q.Y.; Zhang, Q.B.; Cui, M.; Wang, H. Dynamic characteristics and mechanism analysis of 1850 four-high aluminum strip cold rolling mill. *J. Vib. Meas. Diagn.* **2021**, *41*, 991–998. (In Chinese)
7. Evans, P.R.; Vaughan, N.D.; Hill, D.E. Dynamic characteristics of a rolling mill. *J. Syst. Control. Eng.* **1996**, *210*, 259. [CrossRef]
8. Qu, Z.H.; Chai, S.K.; Ye, Q. Analysis of dynamic characteristics and chatter of a 1420 cold tandem rolling mill. *J. Vib. Shock.* **2006**, *25*, 25–29. (In Chinese)
9. Adam, B.; Andrzej, S. Interdependence between the rolling speed and non-linear vibrations of the mill system. *J. Mater. Process. Technol.* **2004**, *155–156*, 2116–2121.
10. Gao, Z.Y.; Bai, L.L.; Li, Q. Research on critical rolling speed of self-excited vibration in the tandem rolling process of thin strip. *J. Mech. Eng.* **2017**, *53*, 118–132. (In Chinese) [CrossRef]
11. Gao, Z.Y.; Yang, L.; Zhang, Q.D.; Liao, M.-L.; Tian, B. Chatter model with structure-process-control coupled and stability analyses in the cold rolling system. *Mech. Syst. Signal Process.* **2020**, *140*, 106692. [CrossRef]
12. Gao, Z.Y.; Zang, Y.; Zheng, L. Review of modelling and theoretical studies on chatter in the rolling mills. *J. Mech. Eng.* **2015**, *51*, 87–105. [CrossRef]
13. Ihuo, Y.; Kusuo, F.; Seino, Y.; Takimoto, T.; Nakazato, Y.; Nakagawa, K. An analysis of chattering in cold rolling for ultrathin gauge steel strip. *Trans. ISIJ* **1978**, *18*, 1–10.
14. Noriki, F.; Yukio, K.; Koji, K.; Kimito, I.; Yosuke, A.; Yasuhiro, S. Dynamic control of lubrication characteristics in high speed tandem cold rolling. *J. Mater. Process. Technol.* **2015**, *229*, 407–416. [CrossRef]
15. Yang, X.; Li, Q.; Tong, C.-N.; Zhang, W.-W. Vertical vibration mechanism analysis of aluminum cold rolling mills based on the dynamic friction equation in roll gap. *J. Univ. Sci. Technol. Beijing* **2014**, *36*, 104–109.
16. Wei, L.Q.; Dai, Z.F.; Xiao, Z.; Qu, Z. Research of vibration and strategy in high-speed cold rolling mill. *J. Mech. Eng.* **2016**, *52*, 89–94. (In Chinese) [CrossRef]
17. Liu, X.C.; Zang, Y.; Gao, Z.; Zeng, L. Multidirectional regenerative chatter model of tandem rolling mills and its application. *J. Cent. South Univ. Sci. Technol.* **2017**, *48*, 635–643. (In Chinese)
18. Liu, H.R.; Zhang, Y.; Shi, P.-M.; Zhao, H.-X. Vibration characteristics of a cold rolling mill with a model of seven degrees of freedom and their influence on dynamic rolling force. *J. Vib. Shock.* **2015**, *34*, 98–102. (In Chinese)
19. Cai, H.; Zhao, L.J.; Shan, L.-J. Dynamic characteristic analysis of hydraulic screw down in cold strip mill. *J. Liaoning Tech. Univ.* **2005**, *24*, 187–189.
20. Peng, Y.; Zhang, Y.; Sun, J.; Zang, Y. Tandem strip mill's multi-parameter coupling dynamic modeling based on the thickness control. *Chin. J. Mech. Eng.* **2015**, *28*, 353–362. [CrossRef]

21. Xu, Y.; Chao, N.T. Coupling dynamic model and control of chatter in cold rolling. *J. Dyn. Syst. Meas. Control.* **2012**, *134*, 041001. [CrossRef]
22. Hou, D.X.; Fang, C.; Chen, S.; Yan, S. Research on hydraulic screw down-vertical vibration characteristics of strip rolling mill. *J. Northeast Univ. Nat. Sci.* **2022**, *43*, 972–980. [CrossRef]
23. Zhu, G.H.; Gao, Y.J.; Pei, L. Study on the influence of strip thickness difference and hardness deviation on the vibration of tandem cold rolling mill. *Metall. Equip.* **2022**, *276*, 23–26. [CrossRef]
24. Sun, Y.K. *Model and Control of Cold and Hot Strip Mill*; Metallurgical Industry Press: Beijing, China, 2010; pp. 57–82.
25. Yang, W.D. Analysis for convergence and steady-state characteristic of GM-AGC. *Metall. Ind. Autom.* **2009**, *11*, 52–68. (In Chinese)
26. Ye, X.H.; Ding, J.J.; Zheng, G.; Jiang, K.; Chen, D. Static and dynamic performance simulation of direct-acting force motor valve. In Proceedings of the 4th International Conference on Mechanics and Mechatronics Research, Xi'an, China, 20–24 June 2017. [CrossRef]


**Disclaimer/Publisher's Note:** The statements, opinions and data contained in all publications are solely those of the individual author(s) and contributor(s) and not of MDPI and/or the editor(s). MDPI and/or the editor(s) disclaim responsibility for any injury to people or property resulting from any ideas, methods, instructions or products referred to in the content.